A UNIFIED VIEW ON THE EFFECT OF FIBERS AND LOADING ON SFRC CREEP THROUGH LINEAR PROJECTION TO LATENT STRUCTURES

EMILI GARCÍA-TAENGUA*, SAMUEL ARANGO*, JOSÉ R. MARTÍ-VARGAS* AND PEDRO SERNA-ROS*

* ICITECH – Institute of Concrete Science and Technology
Universitat Politècnica de València – Camí de Vera, s/n 46022 Valencia, Spain
e-mails: emgartae@upv.es, samo_59@hotmail.com, jrmarti@upv.es, pserna@upv.es

Key words: Flexural Creep, Steel Fiber Reinforced Concrete.

Abstract: Creep of Steel Fiber Reinforced Concrete (SFRC) under flexural loads in the cracked state and to what extent different factors determine creep behaviour are quite understudied topics within the general field of SFRC mechanical properties. A series of prismatic specimens have been produced and subjected to sustained flexural loads. The effect of a number of variables (fiber length and slenderness, fiber content, and concrete compressive strength) has been studied in a comprehensive fashion. Twelve response variables (creep parameters measured at different times) have been retained as descriptive of flexural creep behaviour. Multivariate techniques have been used: the experimental results have been projected to their latent structure by means of Principal Components Analysis (PCA), so that all the information has been reduced to a set of three latent variables. They have been related to the variables considered and statistical significance of their effects on creep behaviour has been assessed. The result is a unified view on the effects of the different variables considered upon creep behaviour: fiber content and fiber slenderness have been detected to clearly modify the effect that load ratio has on flexural creep behaviour.

1 INTRODUCTION

The major feature of steel fiber reinforced concrete (SFRC hereafter) in bending is residual strength, or toughness [1,2]: while conventional unreinforced concrete fails when the first (and only) crack appears, SFRC does not and has a considerable bearing capacity even in its cracked state.

Creep of SFRC under flexural loads in its cracked state, and to what extent different factors determine creep behavior are quite understudied topics within the general field of SFRC mechanical properties. When some of the most relevant research papers and reports [3,4,5,6,7] are brought together, several general aspects arise. There is a great variety of test setups, ratios, parameters, and methodologies. This, added to the fact that SFRCs usually show considerable scatter in their flexural response [8], contributes to the uncertainty about how to characterize their response under sustained flexural loads.

In relation to this, the authors have developed a methodology which has been extensively described elsewhere [9] to make it possible to study flexural creep of concrete in standard-like conditions.

2 SCOPE AND OBJECTIVES

The aim of this research is to study how SFRC flexural creep is affected by a set of variables (geometry of fibers, fiber contents, concrete compressive strength, flexural load).

However, creep behaviour can be looked at through a variety of different measurements and ratios (creep parameters hereafter) which differ in their definition as well as the time spans they cover [10].

This paper reports a profound analysis of SFRC flexural creep response encompassing all creep parameters by means of multivariate techniques.

3 EXPERIMENTAL INVESTIGATION

3.1 The creep test

This research comprised a series of creep tests carried out on pre-cracked prismatic 150x150x600 mm SFRC specimens.

In addition, all batches of concrete were characterized by assessing their compressive strength and flexural behavior [11,12].

A more detailed description of the creep test setup and methodology followed has been already published [9]. First, the specimen is pre-cracked: it is notched and loaded according to the four-point scheme of the standard bending test [11] until the CMOD reaches 0.50 mm. The load corresponding to that crack width, F_w, is retained.

After that, the pre-cracked specimen is subjected to the creep test: the load is kept at a fixed value (this achieved by means of a counterweight) for a certain lapse of time. Specimens have been tested in columns of three according to the setup shown in Figure 1.

3.2 Creep parameters

For each one of the specimens tested, these parameters are defined from the load-CMOD curve obtained (Figure 2 shows an idealized curve for illustration purposes).

They are the following (for further reference, see [3] and [9]):

- *COR(i-14)*, crack opening rate between the initial time and the 14th day.
- *COR(14-30)*, crack opening rate between the 14th and the 30th day.
- *COR (30-90)*, crack opening rate between the 30th and the 90th day.
- *spCOR(i-14)*, specific crack opening rate between the initial time and the 14th day.
- *spCOR(14-30)*, specific crack opening rate between the 14th and the 30th day.
- *spCOR(30-90)*, specific crack opening rate between the 30th and the 90th day.
- $\varphi(14)$, $\varphi(30)$, $\varphi(90)$, creep coefficients at 14, 30, and 90 days, respectively.
- $\varphi_0(14)$, $\varphi_0(30)$, $\varphi_0(90)$, creep coefficients referred to the initial time at 14, 30, and 90 days, respectively.

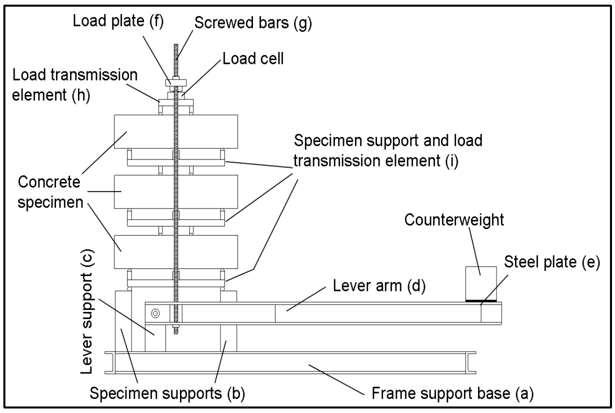

Figure 1: Creep test setup.

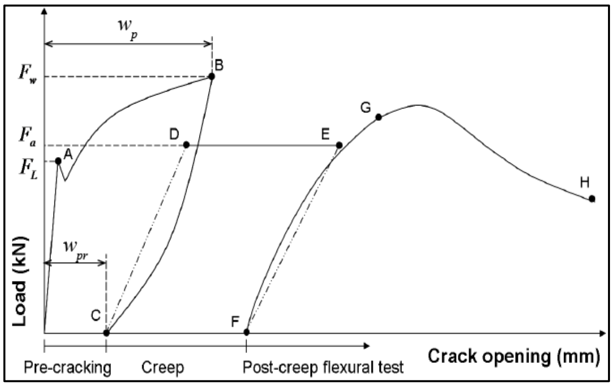

Figure 2: Idealized load-CMOD curve from creep test.

3.3 Variables considered

The variables considered, as well as their different levels, are summarized in Table 1.

Table 1: Variables and levels considered.

Variables	Levels
Base mix design	A (f_c = 40 MPa) B (f_c = 25 MPa)
Fiber slenderness and length, λ_f / L_f	80/35 80/50 65/40 45/50 50/30
Fiber content, C_f	40 kg/m^3 70 kg/m^3
Applied load Ratio, *IFa*	not fixed (*IFn*=60%) not fixed (*IFn*=80%)

Two different base mix designs have been considered: one whose specified compressive strength was 40 MPa (A), the other one being 25 MPa (B), hence covering the range of low and normal strength concretes.

Five different steel fibers have been considered, this resulting in having both fiber slenderness (λ_f) and fiber length (L_f) considered as variables.

Table 2: Combinations tested.

Id.	fc MPa	C_f kg/m^3	λ_f	L_f mm	IFa (%)	Pos.
1	40	40	80	35	60.9	1
2	40	40	80	35	54.9	2
3	40	40	80	35	54.2	3
4	40	40	80	35	97.0	1
5	40	40	80	35	81.9	2
6	40	40	80	35	70.5	3
7	40	70	80	35	61.9	1
8	40	70	80	35	59.2	2
9	40	70	80	35	59.2	3
10	40	70	80	35	81.0	1
11	40	70	80	35	82.2	2
12	40	70	80	35	81.3	3
13	40	40	80	50	79.6	2
14	40	40	80	50	78.8	3
15	25	40	80	50	88.1	1
16	25	40	80	50	82.5	2
17	25	40	80	50	82.2	3
18	25	40	65	40	56.2	1
19	25	40	65	40	60.4	2
20	25	40	65	40	70.8	3
21	25	40	45	50	97.2	1
22	25	40	45	50	80.2	2
23	25	40	45	50	78.3	3
24	25	40	45	50	90.9	1
25	25	40	45	50	84.4	2
26	25	40	45	50	75.1	3
27	25	40	50	30	76.3	1
28	25	40	50	30	57.7	2
29	25	40	50	30	54.4	3
30	25	40	50	30	72.9	2
31	25	40	50	30	72.4	3

Fiber contents (C_f) used are 40 kg/m^3, and 70 kg/m^3, both below the 1% in volume fraction, as it is the case in most of applications using SFRC.

The load ratio determines to what extent the material is loaded in relation to its bearing capacity. The case of load ratio as applied to the specimens (*IFa*) is different from the aforementioned variables because it could not be pre-fixed, since nominal (*IFn*) and applied (*IFa*) load ratio values differ in each case. The nominal load ratio (*IFn*), this could be pre-fixed: it is the ratio between the load applied to the specimen at the top of the specimens column (see Figure 1) and F_w, retained from the pre-cracking stage, in percentage. Two different nominal load ratios have been considered: 60%, and 80%.

Taking all that into consideration, the relative position of each specimen in each group of three might somehow affect the results. This has been taken into account when analyzing the creep parameters so that the effect of the position (Pos. in Table 2) upon them, whenever present, could be substracted in order not to obfuscate the effects of the other variables [10].

4 DETECTION OF OUTLIERS

Outliers have been identified and removed from the dataset before any other analysis is carried out [13].

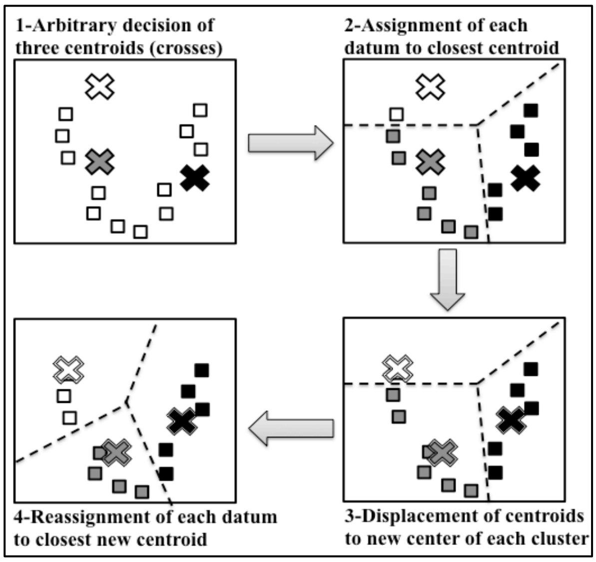

Figure 3: The k-means algorithm exemplified for k=3.

In terms of only one variable, outliers would be unusually high or low values. But in a multivariate context like this, a clustering method must be used instead, namely the k-means algorithm [14], which is a highly visual tool to detect outliers. As illustrated in Figure 3, it partitions the observations into a number of clusters or groups. This way, if a certain observation ends up isolated, forming a group of its own within the 12-dimension set of creep test results, therefore it is clearly an outlier, since it has no similarity whatsoever with other observations.

Only one outlier has been detected and removed (observation no. 30 in Table 3).

5 SEARCH FOR THE LATENT VARIABLES STRUCTURE

5.1 Principal Components Analysis

The search for a latent structure, that is a reduced set of latent variables, or factors, from the set formed by the 12 creep parameters provides: 1) an insight into the relationships among variables, and 2) a simplified, global version of the original information [14].

Principal Components Analysis (PCA) is the method chosen in this case, namely the matrix decomposition procedure known as the Singular Value Decomposition (SVD), because it is the most common procedure for practical purposes [15]. The basis of this method is given by the following equation:

$$\overline{\overline{\mathrm{X}}} = \overline{\overline{\mathrm{U}}}\,\overline{\overline{\mathrm{D}}}\,\overline{\overline{\mathrm{V}}}^{\mathrm{T}} + \overline{\overline{\mathrm{E}}} \qquad (1)$$

Table 3: Complete results from the creep tests carried out.

	COR (E-03)			spCOR (E-03)								
Id.	i-14	14-30	30-90	i-14	14-30	30-90	$\varphi(14)$	$\varphi(30)$	$\varphi(90)$	$\varphi_0(14)$	$\varphi_0(30)$	$\varphi_0(90)$
1	11.2	1.42	0.82	3.44	0.44	0.25	0.598	0.684	0.870	0.297	0.340	0.432
2	10.9	1.22	0.60	3.23	0.36	0.18	0.662	0.746	0.902	0.288	0.325	0.393
3	6.5	0.78	0.34	1.85	0.22	0.10	0.616	0.702	0.839	0.197	0.224	0.268
4	32.8	13.80	1.96	5.58	2.35	0.33	0.601	0.889	1.043	0.443	0.657	0.771
5	26.0	2.67	1.50	4.34	0.45	0.25	0.668	0.746	0.911	0.435	0.486	0.593
6	6.8	1.01	0.58	1.11	0.17	0.10	0.459	0.536	0.706	0.193	0.225	0.297
7	13.3	1.96	0.70	1.96	0.29	0.10	0.668	0.781	0.932	0.362	0.424	0.506
8	17.7	1.63	1.23	2.57	0.24	0.18	0.844	0.932	1.183	0.455	0.502	0.638
9	6.3	0.90	0.46	0.91	0.13	0.07	0.582	0.676	0.856	0.208	0.241	0.306
10	25.8	1.97	1.29	3.35	0.26	0.17	0.585	0.636	0.761	0.415	0.451	0.540
11	28.4	2.08	0.81	3.63	0.27	0.10	0.612	0.663	0.738	0.440	0.477	0.531
12	15.8	1.38	0.58	2.00	0.17	0.07	0.754	0.829	0.947	0.410	0.451	0.515
13	15.6	2.26	1.32	2.85	0.41	0.24	0.478	0.557	0.730	0.309	0.360	0.472
14	15.3	1.56	1.55	2.73	0.28	0.28	0.699	0.780	1.084	0.366	0.408	0.568
15	26.3	4.40	2.45	6.67	1.12	0.62	0.727	0.866	1.156	0.484	0.576	0.770
16	24.0	3.54	1.75	5.91	0.87	0.43	0.837	0.977	1.239	0.479	0.560	0.711
17	19.0	3.01	1.53	4.56	0.72	0.37	1.208	1.427	1.846	0.520	0.615	0.795
18	6.5	1.05	0.75	3.77	0.61	0.44	0.291	0.344	0.489	0.081	0.096	0.137
19	5.4	1.06	0.60	2.97	0.58	0.33	0.345	0.421	0.585	0.117	0.143	0.198
20	7.5	1.49	0.51	3.87	0.77	0.26	0.551	0.675	0.835	0.202	0.247	0.306
21	27.9	1.44	2.34	8.79	0.45	0.74	0.965	1.021	1.368	0.513	0.543	0.727
22	30.2	2.83	3.07	9.19	0.86	0.94	1.182	1.309	1.824	0.592	0.655	0.913
23	14.8	1.82	1.40	4.36	0.54	0.41	1.062	1.211	1.642	0.392	0.448	0.607
24	34.7	5.72	3.21	9.69	1.60	0.90	0.791	0.940	1.253	0.500	0.594	0.792
25	23.7	19.48	3.12	6.41	5.27	0.84	0.940	1.824	2.354	0.464	0.901	1.163
26	19.2	8.82	2.32	5.05	2.32	0.61	1.003	1.529	2.047	0.441	0.672	0.900
27	24.3	3.03	1.84	12.9	1.60	0.97	1.611	1.839	2.360	0.555	0.634	0.814
28	6.7	1.16	0.82	3.36	0.58	0.41	0.742	0.888	1.277	0.184	0.221	0.317
29	5.4	1.28	0.78	2.55	0.61	0.37	0.739	0.940	1.401	0.168	0.214	0.318
30	14.1	46.26	6.43	4.92	16.15	2.24	0.599	2.849	4.022	0.276	1.311	1.850
31	12.3	7.09	4.13	4.16	2.40	1.40	1.070	1.774	3.314	0.328	0.544	1.016

where: X is the original creep test results matrix, D is a diagonal matrix, U and V are orthogonal, rotation matrices, and E is an error matrix. Equation (1) can be understood in the following terms. Test results are data in a 12-dimension space originally expressed in a set of coordinates which is not orthogonal, since the 12 creep parameters are highly correlated. But if such matrix is decomposed according to equation (1), all these data are rewritten in terms of a set of orthogonal, uncorrelated coordinates, each one of them corresponding to a singular value of the matrix $X^T X$.

If all singular values were extracted, then E would be a null matrix. But, since the objective is to simplify the information, only the highest singular values are retained, and then the error matrix E contains the remaining part of the original information.

Prior to the application of PCA to the original dataset of creep test results, all variables have been centered and scaled to unit variance, since they were not homogeneous in their units of measure [14].

The principal components (namely *PC1*, *PC2*,..., *PC12*) obtained are shown in Table 4 together with the corresponding eigenvalues and the percentages of explained variance per component.

Table 4: Eigenvalues, percentage of variance explained by each component and cumulative variance.

	Eigenvalue or variance	Percentage of variance	Cumulative percentage
PC1	8.0969	67.47	67.47
PC2	1.5171	12.64	80.11
PC3	1.2679	10.56	90.67
PC4	0.6959	5.80	96.47
PC5	0.3550	2.96	99.43
PC6	0.0419	0.35	99.78
PC7	0.0150	0.125	99.90
PC8	0.0064	0.053	99.95
PC9	0.0029	0.024	99.98
PC10	0.0009	0.007	99.99
PC11	0.0001	0.001	99.99
PC12	0.0000	0.000	100.00

Emili García-Taengua, Samuel Arango, José R. Martí-Vargas and Pedro Serna-Ros

It can be seen that more than 90% of variance in the original creep parameters is explained with only the three first principal components, which are therefore the only ones retained in this analysis.

Each one of the selected principal components is a linear combination of the 12 original creep parameters. The coefficients of such linear combinations, namely loadings, are given in Table 5.

Table 5: Loadings of initial creep parameters on the selected principal components.

	PC1	PC2	PC3
COR(i-14)	0.2431	**0.5224**	-0.2357
COR(14-30)	0.2446	-0.2447	**-0.5604**
COR(30-90)	0.3146	-0.0609	-0.0426
spCOR(i-14)	0.2677	0.2334	0.1833
spCOR(14-30)	0.2639	-0.3709	-0.3835
spCOR(30-90)	0.2859	-0.2240	0.2173
φ(14)	0.2773	0.0444	**0.4771**
φ(30)	0.3129	-0.2226	0.2252
φ(90)	0.2937	-0.3335	0.2791
φ_0(14)	0.2765	**0.4719**	0.0176
φ_0(30)	0.3244	0.1824	-0.1912
φ_0(90)	0.3410	0.0501	-0.0874

5.2 Linear projection: obtaining the latent variables

Once the three most relevant principal components have been selected, all original data are rewritten in terms of the new, rotated variables, which are the latent variables *LV1*, *LV2*, and *LV3*. The transformed creep test results are given in Table 6.

6 EFFECT OF FIBERS ON CREEP: REGRESSION MODELS

6.1 Overview of the methodology

The effect that the variables considered in this research (see Table 1) have on *LV1*, *LV2*, and *LV3* has been assessed by means of multiple linear regression (MLR hereafter) [13,14,16].

The core of this methodology is building up linear models to relate each latent variable, representing creep strains, to the experimental variables considered. On the basis of such models it is possible to assess which variables have a statistically significant effect on creep response and which ones have not.

Table 6: Creep test results re-expressed in terms of the latent variables chosen.

Id.	LV1	LV2	LV3
1	0.979973	-0.186019	0.5815321
2	1.006095	-0.216228	0.6413448
3	0.858456	-0.257995	0.6221568
4	1.364372	-0.137322	0.5774575
5	1.175825	-0.102928	0.5968666
6	0.733103	-0.184002	0.4692089
7	1.118979	-0.174773	0.6323593
8	1.385543	-0.216913	0.7939476
9	0.867425	-0.249347	0.5980063
10	1.038662	-0.050800	0.5022924
11	1.060729	-0.030094	0.5103900
12	1.187711	-0.156880	0.6826434
13	0.890493	-0.103353	0.4481104
14	1.189751	-0.220800	0.6865328
15	1.406234	-0.160673	0.6878599
16	1.468393	-0.217145	0.7975783
17	1.946081	-0.472166	1.2296110
18	0.436088	-0.160487	0.3221735
19	0.548703	-0.179478	0.3784768
20	0.854250	-0.244747	0.5756109
21	1.566152	-0.247627	0.9081438
22	1.973338	-0.386263	1.1661390
23	1.622947	-0.464754	1.1020160
24	1.497468	-0.189830	0.7546525
25	2.355494	-0.700690	1.2333550
26	2.015099	-0.594860	1.1858320
27	2.364034	-0.692617	1.6535490
28	1.093346	-0.443783	0.8421709
29	1.138060	-0.506564	0.8877888
31	2.447482	-1.143967	1.6413880

6.2 Conceptual basis of the models

Considering that constitutive equations relate applied loads to the response of the material, the linear model for any latent variable (which sums up information regarding strains) has to relate to the load ratio, *IFa*, whose effect can be affected by the other variables considered. As a consequence, the models on which statistical inference is based will follow this general expression:

$$\mathrm{LV_i} = \mathrm{m_i} + (\mathrm{n_i} + \nabla_{\mathrm{f,i}}\mathrm{C_f} + \mathrm{p_i f_c}) \cdot \mathrm{IFa} \qquad (2)$$

where: LV_i is one of the latent variables (i=1,2,3); m_i, n_i, and p_i are constants to be fitted in each case; the term that multiplies *IFa* is affected by compressive strength of concrete, f_c, and fibers, where the fiber content C_f depends on fiber geometry according to the following expression:

$$\nabla_{\mathrm{f,i}} = \nabla_{\mathrm{0,i}} + \nabla_{\lambda,\mathrm{i}}\lambda_{\mathrm{f}} + \nabla_{\mathrm{L,i}}\mathrm{L_f} \qquad (3)$$

where $\nabla_{0,i}$, $\nabla_{\lambda,i}$, and $\nabla_{L,i}$ are constants to be fitted in each case; λ_f is fiber slenderness; and L_f is fiber length.

6.2 Final models obtained and their interpretation

Once all constants have been fitted, those variables which have not a statistically significant effect are detected and removed. Then, the initial model is iteratively simplified and constants are re-estimated to achieve the final models for *LV1*, *LV2*, and *LV3*, i.e. the models that best fit the data and consider only statistically significant variables. The threshold considered for p-values identifying significant effects is 0.05 in all cases [14,16].

Table 7 summarizes these final models. It is very important to notice that, in all cases, only fiber slenderness and fiber content significantly modify the effect that load ratio, *IFa*, has on creep behavior. Furthermore, the fact that all three models obtained follow the same structure reinforces the idea that there was a coherent latent structure within the dataset of creep test results as evaluated by the creep parameters chosen: there exists such a global vision of the phenomenon under study.

Table 7: Fitted coefficients in final models.

	LV1	LV2	LV3
Fitted coefficients for the models			
m_i, intercept	$1.19\cdot10^{-1}$	$-3.85\cdot10^{-1}$	$6.21\cdot10^{-1}$
n_i, IFa	$1.32\cdot10^{-2}$	--	--
$\nabla_{0,i}$, IFa·C_f	$4.45\cdot10^{-4}$	$-1.57\cdot10^{-4}$	$3.47\cdot10^{-4}$
$\nabla_{\lambda,i}$, IFa·$\lambda_f C_f$	$-5.48\cdot10^{-6}$	$2.64\cdot10^{-6}$	$-4.32\cdot10^{-6}$
Overall indicators of the models fitness			
Model significance	0.0011	0.0010	0.0012
R-squared	0.45	0.42	0.39

Figure 4 shows the first latent variable, *LV1*, vs the applied load ratio, *IFa*. It is clear that *LV1* increases when the load ratio is increased.

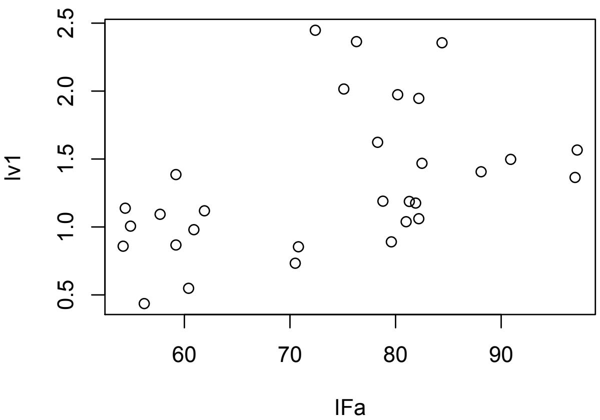

Figure 4: Effect of IFa on LV1.

In relation to fiber content and fiber geometry, similar reasonings can be made for either *LV1*, *LV2*, or *LV3*. Figure 5 shows *LV1* vs the interaction of load ratio with fiber content and slenderness. Considering that *LV1* is the latent variable that explains most of the overall variance in the results (see 5.1 and Tables 4 and 5), it is therefore clear that fibers have a significant effect on the creep performance of the material. Increasing the fiber contents improves the material performance and therefore reduces flexural creep strains for a certain load. And the higher slenderness, the better such improvement is achieved.

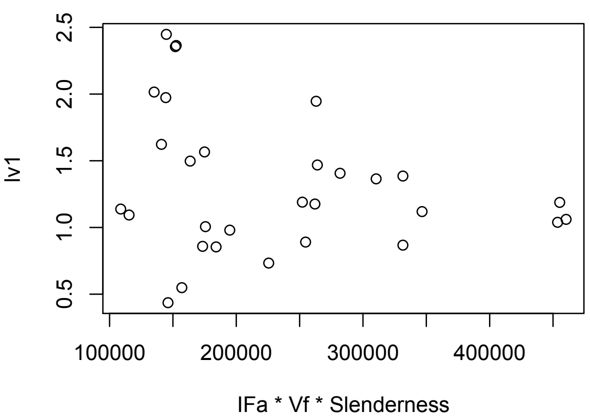

Figure 5: Effect of slenderness on LV1.

7 CONCLUSIONS

More than thirty prismatic specimens of SFRC have been produced, pre-cracked, and tested under sustained bending loads for 90 days.

12 creep parameters that characterize flexural creep behaviour of pre-cracked SFRC have been reduced to a set of only 3 variables which constitute a latent structure explaining flexural creep behaviour in a unified, global way.

The effect of fiber content, fiber geometry, and loading on flexural creep strains has been studied through the 3 latent variables obtained.

Load ratio is the capital factor determining flexural creep strains.

Fiber length has been found to be unsignificant in terms of its effect on flexural creep strains when compared to fiber slenderness.

Fiber slenderness and fiber content significantly modify the effect of the applied load ratio on flexural creep strains.

Higher fiber contents improve the material performance and therefore reduce flexural creep strains for a given load.

Given a load ratio and fiber content, the higher the fiber slenderness the smaller flexural creep strains will be: very slender fibers tend to counteract the tendency of creep strains to increase with load ratio.

REFERENCES

[1] di Prisco, M., Plizzari, G. and Vandewalle, L., 2009. Fibre reinforced concrete: new design perspectives. *Materials and Structures* **42**(9):1261–1281.

[2] Serna, P., Arango, S., Ribeiro, T., Núñez, A., García-Taengua, E., 2009. Structural cast-in-place SFRC: technology, control criteria and recent applications in Spain. *Materials and Structures* **42**(9):1233–1246.

[3] Barragán, B.E., Zerbino, Z.L., 2008. Creep behavior of cracked steel fibre reinforced concrete beams. In *Proc. of the 7th Inter RILEM Symp. on Fibre Reinf. Concrete: Design and Applications (BEFIB 2008)*, Chennai, India; pp.577-

586.

[4] Chanvillard, G., Roque, O., 1999. Behavior of Fibre Reinforced Concrete Cracked Section under Sustained Load. *Proceedings of the 3rd International Workshop on High Performance Fibre Reinforced Cement Composites*, Mainz, Germany; pp. 239-250.

[5] Granju, J.L., Rossi, P., Chanvillard, G., 2000. Delayed Behavior of Cracked SFRC Beams. In *Proceedings of the 5th Inter. RILEM Symp. on Fibre Reinf. Concrete (BEFIB 2000)*, Lyon, France; pp.511-520.

[6] Mackay, J., 2002. *Behavior of Steel and Synthetic Fibre Reinforced Concrete under Flexural Creep Loading*, MSc thesis, Dalhousie University, Canada.

[7] Bast, T., Eder, A., Kusterle, W., 2007. Kriechversuche an Kunststoffmakrofaser-betonen Untersuchungen zum Langzeit-verhalten von Faserbetonen unter Biegezugbeanspruchung - ein Zwischen-bericht, *Faserbeton Beiträge zum qq. Vilser Baustofftag*, pp. 32-35.

[8] Parmentier, B., Vandewalle, L., Van Rickstal, F., 2008. Evaluation of the scatter of the postpeak behaviour of fibre reinforced concrete in bending: A step towards reliability. In: 7th RILEM Symposium on Fibre Reinforced Concrete BEFIB2008. Chennai, India: 2008. p. 133–143.

[9] Arango, S.E., Serna, P., Martí-Vargas, J.R., and García-Taengua, E., 2012. A Test Method to Characterize Flexural Creep Behavior of Pre-Cracked FRC Specimens. *Journal of Experimental Mechanics* **52**(8):1067–1078.

[10] Arango, S., García-Taengua, E., Martí-Vargas, J.R., Serna-Ros, P., 2012. A Comprehensive Study on the Effect of Fibers and Loading on Flexural Creep of SFRC. In *Proceedings of the 8th Inter. RILEM Symp. on Fibre Reinf. Concrete (BEFIB 2012)*, Guimaraes, Portugal; pp.173–174.

[11] European Standard EN 14651:2007. *Test method for metallic fibre concrete - Measuring the flexural tensile strength (limit of proportionality (LOP), residual)*, European Committee for Standardization.

[12] European Standard EN 12390-3:2009. *Testing hardened concrete - Part 3: Compressive strength of test specimens*, European Committee for Standardization.

[13] Montgomery, D., 2005. *Design and Analysis of Experiments*, 6th edition, John Wiley & Sons, Inc., New York, 643 pp.

[14] Hair, F., Black, W., Babin, B., Anderson, R., 2009. *Multivariate Data Analysis*, 7th edition, Prentice Hall, 816 pp.

[15] Wold, S., Esbensen, K. and Geladi, P., 1987. Principal component analysis. *Chemometrics and Intelligent Laboratory Systems* **2**(1-3):37–52

[16] Draper, N., Smith, H., 1981. *Applied Regression Analysis*, John Wiley & Sons, New York.